Determination of Protein Amount in Nanosized Synthetic Liposomes by Surface Enhanced Raman Spectroscopy (SERS)

Şeyma Parlatan [1*]

[1]Istinye University, Vocational School of Health Services, TR-34010, Zeytinburnu, Istanbul, Türkiye

Abstract − Accurate characterization of synthetic liposomes is essential since they give information about the vesicular structures in bodily fluids such as extracellular vesicles. The characterization tasks are generally the determination of the sizes of the liposomes and the profiling of the liposomes' content. Optical tweezers and Surface Enhanced Raman Spectroscopy (SERS) were used to profile the nanosized liposomes. The size distribution of the trapped liposomes (140 nm on average) was found by using Einstein's Brownian motion equation, consistent with the size distribution obtained from dynamic light scattering measurements. Besides, Gramicidin-encapsulated liposomes were measured using SERS, and statistically significant differentiation was found in Raman intensities between liposome populations with altering concentrations of proteins. This study uniquely measured size distributions of nano-sized liposomes with conventional optical tweezers (without plasmonics) and determined the chemical differences between empty and protein encapsulated liposomes with high accuracy using Raman spectroscopy.

1. Introduction

Liposomes are microscopic vesicles enclosing a liquid inner chamber in one or more lipid bilayer layers (lamella). These structures are biocompatible and biodegradable and do not produce an immune response (Laouini et al., 2012). Although it consists of amphiphilic phospholipid molecules, different biomolecules (functional group-linked phospholipid, cholesterol, cell membrane protein, etc.) are added to their structures, such as bioactive substance (drug, vaccine, gene) transport systems. They are widely used in various fields, including protein structure-function relationships and protein-lipid interactions (Laouini et al.,2012; Zhang,2017). Efficiency and success in use areas depend on the liposome's structure and properties. The structure and properties of liposomes vary significantly according to their molecular contents, sizes, number of layers, charges, and the way they are formed (Alavi et al., 2017, Akbarzadeh et al., 2013). The diameters of liposomes range from 20 nm to a few µm. They can be classified in to different classes due to their number of layers, small-single-layer (20-100 nm), large-monolayer (>100 nm), very large-monolayer (>1000 nm), and multilayer (> 500 nm). Using monolayer liposomes allows the entrapped molecules to be uniformly stored in a single fluid compartment (Alavi et al., 2017). There are four different phospholipids commonly used in liposome construction. These are PC: Phosphocholine, DPPC: 1,2-dipalmitoyl-sn-glycero-3-phosphocholine, DMPC: 1,2-dimyristoyl-sn-glycero-3-phosphocholine, DLPC: 1,2-dilauroyl -sn-glycero-3-phosphocholine can be listed as DOPC 1,2-dioleoyl-sn-glycero-3-phosphocholine. After G. Gregoriadis (Gregoriadis & Ryman, 1971) proposed that liposomes for use as a drug delivery system, liposome studies advanced technological developments in various fields, especially in mathematics, theoretical physics, biophysics, chemistry, biochemistry, and biology disciplines. With the contribution of new methods and different fields,

---

[1] seyma.parlatan@istinye.edu.tr

*Corresponding Author

many developments such as remote drug loading, extrusion for homogeneous measurements, construction of long-circulation liposomes, and the development of liposomes containing nucleic acid polymers and liposomes containing drug combinations have emerged (Allen & Cullis, 2013) As they can also create model structures for exosomes, liposomes have proven to be very useful in processes that are difficult to understand.

The method used in this study to examine liposomes is optical tweezers. Optical tweezers is a method that was awarded the Nobel Prize in 2018 (Ashkin, 1997) and is based on the principle of momentum transfer to a micrometer or nanometer-sized particles by tightly focusing laser beams with the help of high numerical aperture lenses (Neuman & Block, 2004; Ashkin, 1997). Numerous applications of optical tweezers have been demonstrated over the years. In general, it has been found that this method enables a biological particle to remain undamaged in its environment for a long time, and position measurement allows measurement of optical forces. In one of these applications, studies were carried out using the escape force method utilizing particles with a diameter of 1 µm via optical tweezers (Simon & Libchaber, 1992). In another study, direct observation by optical tweezers of the step movements of kinesin found kinesins to move in 8-nm steps (Svoboda et al., 1993). In addition, the optical tweezers system allowed the mechanical properties of polymers and biopolymers to be studied. The mechanical properties were observed to be consistent with the conventional muscle contraction model (Finer et al., 1994). Optical tweezers have been used to study living systems and biomolecules as well as model systems such as liposomes (cell membrane, exosome, etc.). One of the most interesting applications of these is the use of liposomes produced by the reversible phase evaporation method as a micro-chemistry laboratory with optical tweezers (Kulin et al.,2003). In this study, liposomes containing different types of optically trapped chemicals are combined systematically, and a chemical reaction is initiated with the mixture of their contents. Thus, it can be used as a micro-reactor. In another study, Foo et al. (Foo et al., 2003) showed that phosphatidylcholine liposomes are significantly deformed due to hydrodynamic forces. The mechanical properties of giant liposomes were demonstrated by using the dual optical tweezers method and the optical measurement of force constants by stretching the liposomes (Shitamichi et al., 2009). In two different studies conducted in 2011 and 2014, the chemical transport properties of liposomes, which have an important place in drug targeting, were examined in a controlled manner with the help of optical tweezers (Pinato et al., 2011; Shiomi et al., 2014).

Optical tweezers can also be combined with other analysis methods to examine various properties of trapped particles. Raman spectroscopy was utilized in this study since it is suitable for examining molecular properties of biological particles. In Raman spectroscopy, light scattering occurs by molecules when a monochromatic light from an illumination source interacts with the molecules in the structure of the illuminated sample and results in a fingerprint signal specific to the molecules inside the sample of interest. Many essential studies and applications have been made in biology and medicine with Raman spectroscopy. A study visualized the relationship of living cells with DNA with phosphate stretch vibration and proteins with amide I vibration (Cheng et al., 2002). Besides, water with OH stretch vibration (Dufresne et al.,2003) and lipidic reactions with CH stretch vibration have been observed (Nan et al.,2006). In addition to these studies, vibrational imaging of bilayer lipids has been achieved (Potma & Xie, 2003). Raman scattering has also created a powerful imaging method to study tissues in living organisms (Evans et al., 2005). Cherney and his team examined liposomes of 0.6 µm (Cherney et al., 2003) and 3 µm in diameter (Cherney et al., 2004) produced from different types of phospholipids (DMPC, DPPC, DLPC, DOPC) by Raman tweezers method in two studies conducted in 2003 and 2004. Following this study, extensive studies were conducted with particles 0.5 µm in diameter and above with Raman tweezers (Hotani et al., 1999; Spyratou et al.,2015; Penders et al.,2018; Chan et al., 2005). Raman tweezers studies were also carried out by producing liposomes with diameters between 50 and 200 nm at submicron scale. In one of them, Kruglik trapped 50, 100, 200, and 400 nm liposomes to model the exosome behavior and studied Raman spectra (Kruglik et al., 2019). In this study, Kruglik determined the concentrations of these liposomes using the spectral ratios of CH_2 (1440) and H_2O (1640) bond strengths.

Since spontaneous Raman is a method produces a weak signal, an amplification mechanism is necessary to extract information from the nanosized particles, which contains low volume of material, generally not sufficient to obtain observable spectra. We propose to apply Surface Enhanced Raman Spectroscopy (SERS), a special form of Raman spectroscopy to enhance molecular vibrations by matching the incident electromagnetic wave's frequency with the localized surface plasmons resonance frequency which occurs very

close to the metal surface (5-40 nm) (Stiles et al.,2008). Recently, it has been investigated how SERS efficiency increases with aptamer (Kim et al.,2010), gold nanostar (Lee et al.,2014), nanorod (Chaney et al., 2005), nanoshell (Jackson et al.,2003), nanoparticle (Kneipp et al.,2002) doped applications. Metal nanoshells are a class of nanoparticles with tunable optical resonances. In the article (Hirsch et al., 2003) an application of this technology to thermal ablative therapy for cancer is described. In another article, they carried out the first measurements of a solid-supported lipid bilayer on a SERS-active substrate and characterized the bilayer using SERS, atomic force microscopy, surface plasmon resonance spectroscopy, ellipsometry, and fluorescence recovery after photobleaching (Bruzas,2019).

In this study, optical tweezers and SERS were applied to determine the size distributions of the vesicles and the amount of proteins inside PC liposomes. To our knowledge, this is the first application of SERS-tweezers on quantification of proteins in lipid nanovesicles. This study especially important for being a model for extracellular vesicle studies, which became quite impactful in the area of cancer research.

2. Materials and Methods

2.1. Generation of AuNP-free liposomes

A thin lipid film was formed to form AuNP-free liposomes (Kılıç,2017). For this, 40 µL of the phosphatidylcholine (PC, Figure 1A) stock solution (2.5 mg/mL) prepared in chloroform was poured into a round-bottomed flask (100 mL), and a thin film was formed by evaporating the chloroform under nitrogen gas by manually rotating it. Large, multilamellar liposomes (Large Multilamellar Vesicles, LMV) were then obtained by vigorously mixing the lipid layer by vortexing for 15 minutes in phosphate buffer (PBS; pH: 7.4 and 0.01 M).
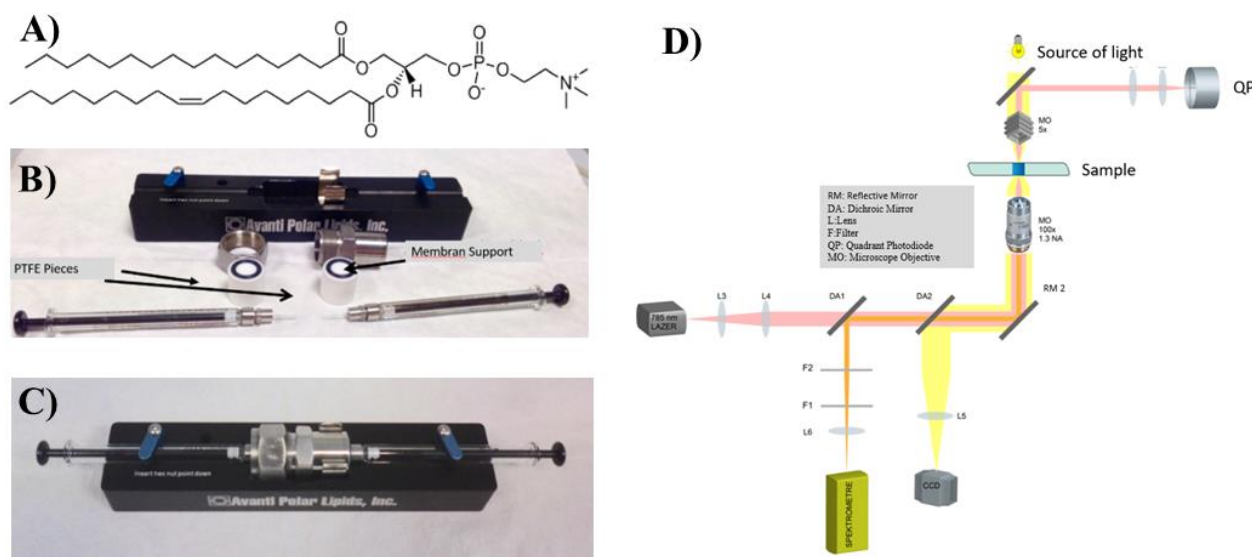

Figure 1. A)Structure of the phosphatidylcholine molecule. B) Mini extruder system components and C) combined view. D) Raman tweezers experimental setup.

The extrusion method was used to obtain a monolayer liposome (Small Unilamellar Vesicles, SUV) (Avanti Mini-Extruder, Figures 1-B and 1-C). For this, the LMV solution was passed through the polycarbonate membrane placed in the center of the extrusion system 21 times with syringes on both sides. Membranes with different pore sizes (50-1000 nm) were used to form liposomes of different sizes. The resulting LMV or SUV liposomes were stored in the falcon at +4 ºC and used within 1-3 days after production (Kılıç & Kok, 2019).

2.2. Experimental setup

The Raman tweezers experimental setup, in which the liposomes are characterized, is given in Figure 1D and is basically built around a 785 nm, 500 mW single-mode diode laser, spectrometer, and microscope. In the

experimental setup, the 785 nm laser beam is directed to the microscope objective with the help of suitable lenses and reflective mirrors. The laser beam focused through the microscope objective (100x, 1.3 NA) reaches the sample. The rays passing through the sample reach the quadrant photodiode with the help of a reflective mirror (RM1) and lenses (L1, L2). The beams emitted from the white light source pass through the sample using lenses (L) and reach the CCD camera via the dichroic mirror (DA 2). Since the dichroic mirror (DA 2) has a long pass filter allowing beams with wavelengths larger than 650 nm, visible light below 650 nm is reflected. This beam is imaged on the camera as light with a wavelength greater than 650 nm passes through the mirror. The rays scattered from the sample are delivered to the spectrometer with the help of a reflective mirror (RM 2), dichroic mirror (DA 1), and filters (F1, F2). Since the dichroic mirror (DA1) has the property of transmitting wavelengths shorter than 805 nm, light above 805 nm wavelength is reflected and directed towards the spectrometer. Since the Raman scattering lights will have a wavelength above 785 nm, only Raman scattering beams reach the spectrometer.

2.3. Raman tweezers characterization of produced liposomes

The Raman spectra were acquired 14 times with a 30-second signal acquisition time for Raman, and the time average of the spectra was taken. The averaged spectra were normalized after baseline and background correction preprocessing and the statistical analysis was started. The signal collection time was planned to be 2 seconds in the SERS application.

3. Results and Discussion

3.1. Tweezers calibration with 5 µm silicon beads

In optical tweezers experiments, calibration experiments are performed to qualitatively determine the magnitude of the optical force transferred to the laser tweezer particles. The calibration experiments find the size of the spring constant in the optical tweezers force, which conforms to Hooke's law. Thus, the change in optical force can be recorded by monitoring the center of mass changes. For silica beads with a diameter of 5 µm, a linear variation of the spring constant versus laser power results from repeated calibration. The spring constant of the system depends on the laser power, where $= 0.16075. P + 3.7 \, pN/\mu m$.

Here the power values are the percentage values relative to the highest power reaching the sample plane. In the preliminary study, the system was gradually calibrated up to 100 nm, starting from test particles with a diameter of 5 micrometers, then readied for calibration of the forces acting on the nanometer-sized liposomes.

By adding Quadrant Photodetector (QPD) to the system, the Brownian motion of the particle in the sample plane was followed by voltage information based on the method known as back focal plane interferometry (back focal plane interferometry) in the literature. Since the commercial system allows the movement of the laser focus in a controlled manner, the voltage-position (V-X) relationship was found by moving a trapped particle linearly throughout the entire observation area (Figure 2A). When the linear region marked in blue in this graph is fit, the beta coefficient, which is directly related to the spring constant of the optical force, is obtained (Figure 2B).

3.2. Multilayer liposome measurements

The sample was prepared with liposomes called large multilamellar vesicles (LMV), and the Brownian motion of particles 1-3 µm in diameter was measured. As a result of two different experiments, spring constants of 80-100 mW (Figure 2C) and then 40-70 mW (Figure 2D) were found. The size values of the measured liposomes were measured with the aid of a CCD camera using the device software. Experiments were continued by taking measurements from a region with no visible particles and observing that there was no voltage change. In addition, the Stokes-Einstein (1) diffusion equation given in equation 1 was used to determine the diameters of the trapped particles:
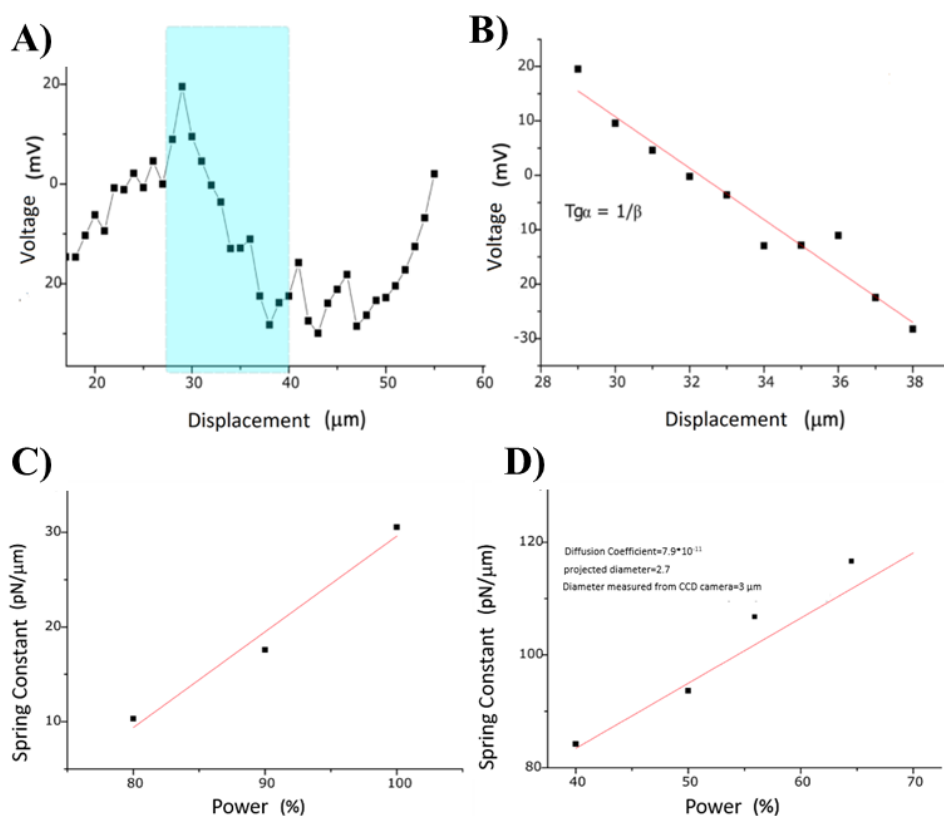
$$D = \frac{k_B T}{\gamma} \tag{3.1}$$

Figure 2. Calibration with QPD A) Voltage-displacement curve B) Linear fit on the selected region. Spring constant vs laser power calibration were measured for C) small unilamellar vesicles D) large multilamellar vesicles.

Here, k_B, T, and γ are Boltzmann's constant ($m^2.kg.s^{-2}.K^{-1}$), ambient temperature (K), and fluid friction coefficients, respectively. (m.Pa.s). Since $\gamma = 6\pi r\eta$, the radius r value can be left alone and the fitted D value can be used. The open source optical tweezers power spectrum fit program named CPC package was used for the fit process (Hansen et al., 2006; Tolić-Nørrelykke et al.,2004).

3.3. Monolayer liposome measurements

Preliminary studies continued with experiments at SUVs with an average diameter of 100 nm. At this stage, since the particles cannot be seen with the naked eye under the microscope (due to the diffraction limit), voltage signals were followed, and the entry of the particles into the trap was indirectly investigated. Figure 3A and B shows the position signal distribution from QPD with and without particles in the trap. The variance decreases dramatically when the particle enters the trap. In the first case, the variance was 2.1055e-16, with the particle in the trap was 1.9936e-17.
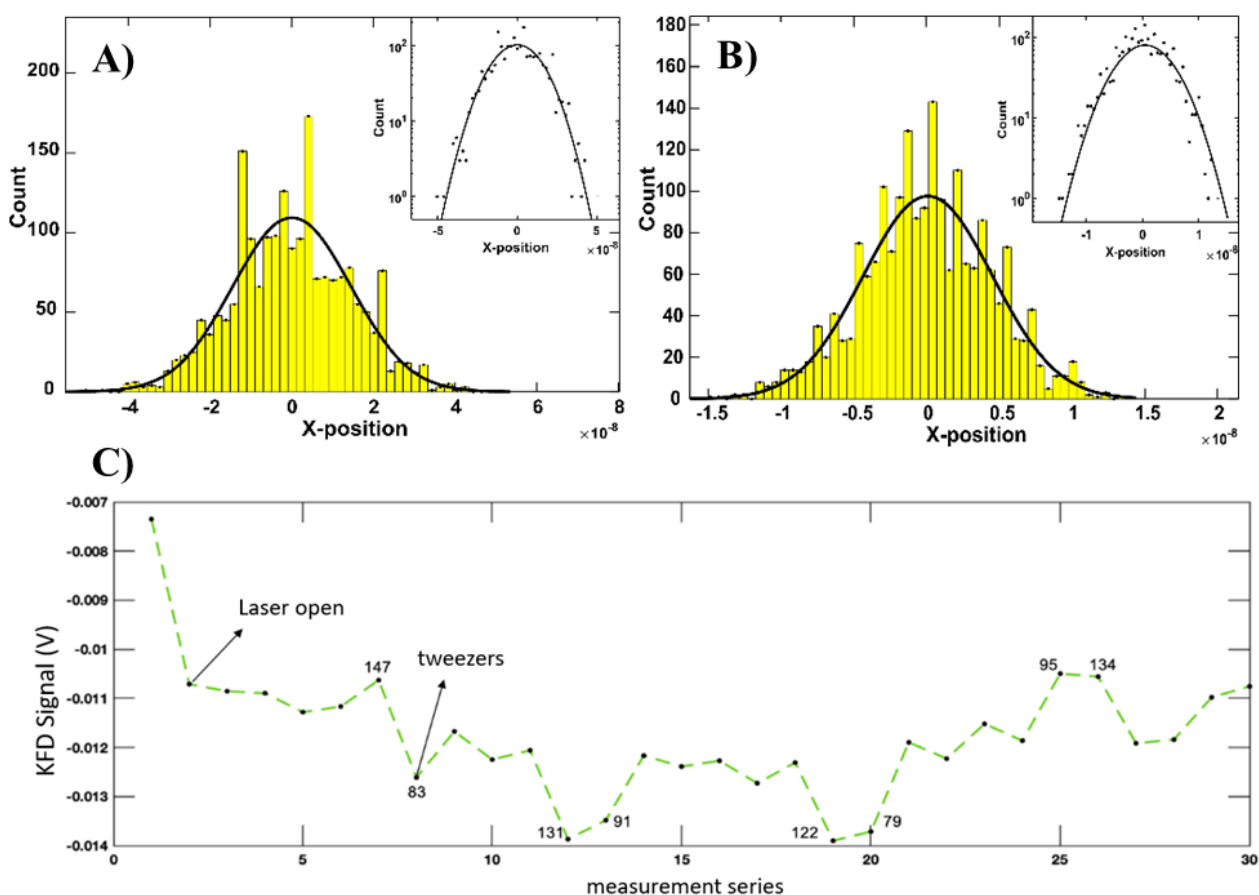
Figure 3. Position distribution with particle A) absent and B) present in the trap. C) Graph of calculated signal averages for understanding tweezers events.

150 consecutive oscilloscope recordings were made for each measurement. In the first recording, noise measurements were taken when the devices and lashe trapping ever were turned off. In the second recording, the devices and laser were turrned on with no trap. In the third measurement, the trapping events were were recorded using the averages of five and the QPD voltage signal was compared with the measurement taken when the laser was turned on (t=0). Figure 3C shows the average signal graph described.

By using corner frequencies and diffusion coefficients obtained as a result of Brownian motion tracking of liposomes, spring constant and estimated diameter values were obtained as in previous experiments. Estimated diameter values are given in nm around the data points on Figure 4. The spring constant value was found to be $11.98 \pm 0.57 pN/\mu m$ against 80% laser power. Figure 4 gives the diameter distributions obtained in optical tweezers studies of the liposomes produced with membranes with a pore diameter of 100 nm. Accordingly, the peak of the distribution obtained was around 140-150 nm, which is in agreement with the 140 nm result obtained previously as a result of the zeta-sizer measurement with the same type of membranes.
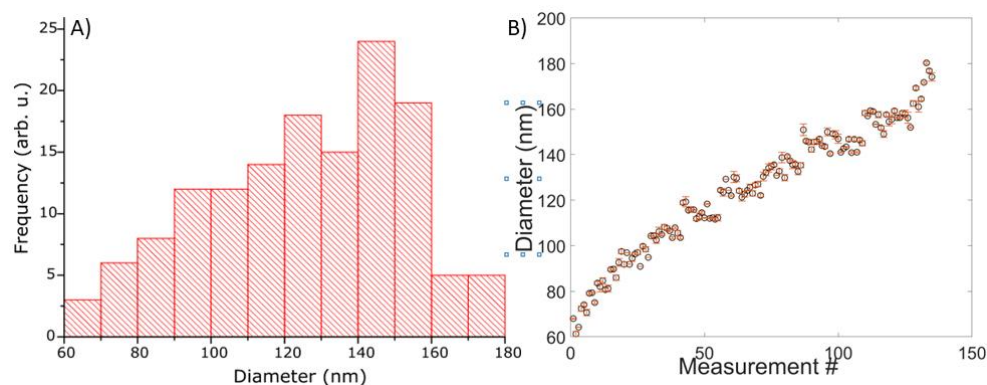
Figure 4. a) Histogram for diameter distributions of liposomes obtained with optical tweezers, 100 nm pore diameter membrane. b) Averages and standard errors of individual vesicle measurements.

SERS spectra of the liposomes produced in the study were also obtained. The surface plasmon resonance wavelength 785 nm obtained from Oceans was measured by drying 15 µL liposome samples on gold surfaces and measured using Oceans QE Raman spectrometer in a similar setup as in Figure 1D, with collection times of 3 seconds. Since it is not possible to determine in which regions the liposomes bind on the surface with optical imaging (Liposome diameters are smaller than the diffraction limit of our microscope, which is 740 nm), a Raman map was obtained by scanning a 1.4 mm X 1.4 mm region on the surface. A model protein, Gramicidin, was used to test the potential of Raman microscopy to distinguish liposomes containing different biomolecules. The analyses performed by producing 1% and 10% Gramicidin-containing liposomes by volume determined that liposomes with and without Gramicidin showed different properties. Analysis results are given in Figure 5 B-D. Figure 5B and C shows that the classification accuracy is high, and the analysis showed 20 misclassified measurements among 3888 measurements taken from three different groups. Fig 5D also confirms that the principal components' distribution is well-clustered, with minor in-group variances and large between-group variances, which provided the accuracy we obtained from the analysis.
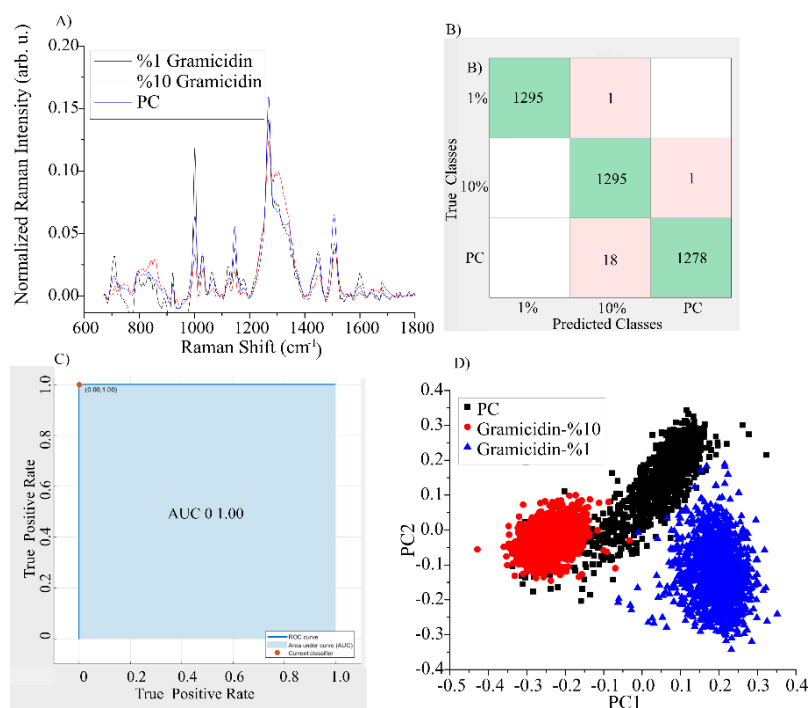

Figure 5. A) Comparison of Raman signals of averaged and L2 normalized PC liposome and liposomes containing 1% and 10% Gramicidin protein. B) Confusion table for test results after LDA analysis. C) ROC plot for LDA analysis. The area under the curve = 1.00. D) Principal component analysis (PCA) comparison of groups.

In this study, the size distribution of the vesicles was determined by optical tweezers using Einstein's diffusion coefficient equation utilizing the displacements of the individual particles inside the trap. This technique was demonstrated for the determination of trap stiffness (Gieseler et al.,2021, Viana et al., 2007, Singer et al., 2000) and the calculation of cell biomechanics (Serafetinides et al.,2013, Pesen et al., 2022, Zhang et al., 2019) before. To the author's knowledge, this is the first demonstration of the estimation of nanoliposomes' diameters by optical tweezers. Besides, the content of the vesicle was analyzed by surface-enhanced Raman spectroscopy. The author found that the signal from the lipid bilayer could be differentiated from the total liposome signal with protein with 1% and 10% concentration. As demonstrated before (Tukova et al., 2021), SERS analysis is sensitive in investigating liposome-protein systems. Here, the author presents a workflow to fully characterize nano-vesicles via SERS-tweezers, which paves the way towards label-free integrated extracellular vesicle analysis, which is important for cancer research.

4. Conclusion

Characterization of nanosized vesicles smaller than 200 nm is challenging due to their small sizes, which is a limitation for optical methods due to the diffraction limit. Besides, the non-optical methods are generally low-throughput and generally do not give sensitive content information. Our Raman tweezers approach brought three advantages: i) The size distribution is sensitively measured using Brownian motion. ii) Content of the nanosized liposomes was measured using Raman spectroscopy. iii) With the help of machine learning methods, untrained protein concentrations can be potentially calculated. These synthetic vesicle measurements have the potential to simulate the extracellular vesicles, especially exosomes, present in the bodily fluids. Since the precise characterization of the exosomes are crucial for cancer diagnosis, a model experiment is highly important and our method shows that the controllable addition of cargo contents into sytentic liposomes and their Raman measurements may provide more accurate cancer diagnosis platforms.

Acknowledgement

Author Contributions

Şeyma Parlatan: Planning of the study, data collection and analysis, statistical analysis and article writing

Conflicts of Interest

The author declares no conflict of interest.

References

Akbarzadeh, A., Sadabady, R.R., Davaran, S., Joo, S. W., Zarghami, N., Hanifehpour, Y., Samiei, M., Kouhi, M., Nejati-Koshk, K., (2013). Liposome: classification, preparation, and applications. *Nanoscale research letters,* 8(1), 1-9. Retrieved from: https://doi.org/10.1186/1556-276X-8-102

Alavi, M., Karimi, N., Safaei, M., (2017). Application of various types of liposomes in drug delivery systems. *Advanced pharmaceutical bulletin*, 7(1), 3-9, Retrieved from: https://doi.org/ 10.15171/apb.2017.002

Allen, T.M., Cullis, P.R, (2013). Liposomal drug delivery systems: from concept to clinical applications. *Advanced drug delivery reviews,*65(1), 36-48. Retrieved from: https://doi.org/10.1016/j.addr.2012.09.037

Ashkin, A., (1997). Optical trapping and manipulation of neutral particles using lasers. *Proceedings of the National Academy of Sciences,* 94(10), 4853-4860. Retrieved from: https://doi.org/10.1073/pnas.94.10.4853

Bruzas, I., Brinson, B. E., Gorunmez, Z., Lum, W., Ringe, E., & Sagle, L. (2019). Surface-enhanced Raman spectroscopy of fluid-supported lipid bilayers. ACS applied materials & interfaces, 11(36), 33442-33451.

Chan, J.W., Winhold, H., Lane, S.M., Huser, T., (2005). Optical trapping and coherent anti-Stokes Raman scattering (CARS) spectroscopy of submicron-size particles. *IEEE Journal of selected topics in quantum electronics,* 11(4), 858-863. Retrieved from: https://doi.org/10.1109/JSTQE.2005.857381

Chaney, S.B., Shanmukh, S., Dluhy, R.A., Zhao, Y.P., (2005). Aligned silver nanorod arrays produce high sensitivity surface-enhanced Raman spectroscopy substrates. *Applied Physics Letters*, 87(3), 031908. Retrieved from: https://doi.org/10.1063/1.1988980

Cheng, J.-X., Jia, Y.K., Zheng, G., Xie, X. S., (2002). Laser-scanning coherent anti-Stokes Raman scattering microscopy and applications to cell biology. *Biophysical journal*, 83(1), 502-509. Retrieved from: https://doi.org/10.1016/S0006-3495(02)75186-2

Cherney, D.P., Conboy, J.C., Harris, J.M., (2003). Optical-trapping Raman microscopy detection of single unilamellar lipid vesicles. *Analytical chemistry*, 75(23),6621-6628. Retrieved from:https://doi.org/10.1021/ac034838r

Cherney, D.P., Bridges, T.E., Harris, J.M., (2004). Optical trapping of unilamellar phospholipid vesicles: investigation of the effect of optical forces on the lipid membrane shape by confocal-Raman microscopy. *Analytical chemistry*, 76(17), 4920-4928. Retrieved from: https://doi.org/10.1021/ac0492620

Dufresne, E.R., Corwin, E. I., Greenblatt, N. A., Ashmore, J.,Wang, D. Y. , Dinsmore, A. D., Cheng, J. X., Xie, X. S., Hutchinson, J. W., Weitz, D. A.,(2003). Flow and fracture in drying nanoparticle suspensions. *Physical review letters*, 91(22), 224501. Retrieved from: https://doi.org/10.1103/PhysRevLett.91.224501

Evans, C.L., Potma, E.O., Puoris'haag, M., Xie, X.S., (2005). Chemical imaging of tissue in vivo with video-rate coherent anti-Stokes Raman scattering microscopy. *Proceedings of the national academy of sciences,* 102(46),16807-16812. Retrieved from: https://doi.org/10.1073/pnas.0508282102

Finer, J.T., Simmons, R.M., Spudich, J.A., (1994). Single myosin molecule mechanics: piconewton forces and nanometre steps. *Nature,* 368(6467), 113-119. Retrieved from: https://doi.org/10.1038/368113a0

Foo, J.-J., Liu, K.-K., Chan, V., (2003). Thermal effect on a viscously deformed liposome in a laser trap. *Annals of biomedical engineering*, 31(3), 354-362. Retrieved from: https://doi.org/10.1114/1.1555626.

Gieseler J., Gomez-Solano J. R., Magazzù A., Castillo I. P., Laura Pérez García, Marta Gironella-Torrent, Xavier Viader-Godoy, Felix Ritort, Giuseppe Pesce, Alejandro V. Arzola, Karen Volke-Sepúlveda, and Giovanni Volpe, "Optical tweezers — from calibration to applications: a tutorial," Adv. Opt. Photon. 13, 74-241 (2021)

Gregoriadis, G., Ryman, B., (1971). Liposomes as carriers of enzymes or drugs: a new approach to the treatment of storage diseases. *Biochemical Journal*, 124(5),58P-58P. Retrieved from: https://doi.org/10.1042/bj1240058p

Hansen,P.M., Tolić-Nørrelykke, I.M., Flyvbjerg, H., Berg-Sørensen, K., (2006). tweezercalib 2.0: Faster version of MatLab package for precise calibration of optical tweezers. *Computer physics communications*, 174(6), 518-520. Retrieved from: https://doi.org/10.1016/j.cpc.2005.11.007

Hirsch, L.R., Stafford, R.J., Bankson, J.A., Sershen, S.R., Rivera, B., Price, R.E., Hazle, J.D., Halas, N.J., West, J.L., (2003) Nanoshell-mediated near-infrared thermal therapy of tumors under magnetic resonance guidance, 100 (23) 13549-13554, Retrieved from: https://doi.org/10.1073/pnas.2232479100

Hotani, H., Nomura, F., Suzuki, Y., (1999). Giant liposomes: from membrane dynamics to cell morphogenesis. *Current opinion in colloid & interface science*, 4(5), 358-368. Retrieved from: https://doi.org/10.1016/S1359-0294(99)90021-3

Jackson, J.B., Westcott, S.L., Hirsch, L.R., West, J.L., Halas,N.,J., (2003). Controlling the surface enhanced Raman effect via the nanoshell geometry. *Applied Physics Letters*, 82(2), 257-259. Retrieved from: https://doi.org/10.1063/1.1534916

Kılıç A., Kok, F.N., (2019). Peptide-functionalized supported lipid bilayers to construct cell membrane mimicking interfaces. *Colloids and Surfaces B: Biointerfaces*, 176, 18-26. Retrieved from:

https://doi.org/10.1016/j.colsurfb.2018.12.052

Kılıç, A., Jadidi, M.F., Özer, H. Ö., Kök, F.N., (2017). The effect of thiolated phospholipids on formation of supported lipid bilayers on gold substrates investigated by surface-sensitive methods. *Colloids and Surfaces B: Biointerfaces,* 160, 117-125. Retrieved from: https://doi.org/10.1016/j.colsurfb.2017.09.016

Kim, N.H., Lee, S.J., Moskovits, M., (2010). Aptamer-mediated surface-enhanced Raman spectroscopy intensity amplification. *Nano letters*, 10(10), 4181-4185. Retrieved from: https://doi.org/10.1021/nl102495j

Kneipp, K., et al., (2002). Surface-enhanced Raman spectroscopy in single living cells using gold nanoparticles. *Applied Spectroscopy*, 56(2),150-154.

Kruglik, S.G., et al., (2019). Raman tweezers microspectroscopy of circa 100 nm extracellular vesicles. *Nanoscale*, 11(4), 1661-1679. Retrieved from: https://doi.org/10.1039/C8NR04677H

Kulin, S., Kishore, R., Helmerson, K., Locascio, L., (2003). Optical manipulation and fusion of liposomes as microreactors. *Langmuir*, 19(20), 8206-8210. Retrieved from: https://doi.org/10.1021/la0344433

Laouini, A., Jaafar-Maalej, C., Limayem-Blouza, I., Sfar, S., Charcosset, C., Fessi, H., (2012). Preparation, characterization and applications of liposomes: state of the art. *Journal of colloid Science and Biotechnology,*. 1(2), 147-168. Retrieved from: https://doi.org/10.1166/jcsb.2012.1020

Lee, J., Hua, B., Park, S., Ha, M., Lee, Y., Fan, Z., Ko, H., (2014). Tailoring surface plasmons of high-density gold nanostar assemblies on metal films for surface-enhanced Raman spectroscopy. *Nanoscale,* 6(1), 616-623. Retrieved from: https://doi.org/10.1039/C3NR04752K

Nan, X., Potma, E.O., Xie, X.S., (2006). Nonperturbative chemical imaging of organelle transport in living cells with coherent anti-stokes Raman scattering microscopy. *Biophysical journal,* 91(2), 728-735. Retrieved from: https://doi.org/10.1529/biophysj.105.074534

Neuman, K.C., Block, S.M., (2004). Optical trapping. *Review of scientific instruments,* 75(9), 2787-2809. Retrieved from: https://doi.org/10.1063/1.1785844

Pesen, T., Haydaroglu, M., Capar, S., Parlatan, U., & Unlu, M. B. (2022). Comparison of the human's and camel's erythrocyte deformability by optical tweezers and Raman spectroscopy. bioRxiv, 2022-08.

Penders, J., Pence, I.J., Horgan, C.C., Bergholt, M.S., Wood, C.S., Najer, A., Kauscher, U., Nagelkerke, A. and Stevens, M.M., (2018). Single particle automated raman trapping analysis. *Nature communications*, 9(1), 1-11.

Pinato, G., Raffaelli, T., D'Este, E., Tavano, F., & Cojoc, D. (2011). Optical delivery of liposome encapsulated chemical stimuli to neuronal cells. *Journal of biomedical optics,* 16(9), 095001-095001. Retrieved from:https://doi.org/10.1117/1.3616133

Potma, E. O., Xie, X. S., (2003). Detection of single lipid bilayers with coherent anti-Stokes Raman scattering (CARS) microscopy. *Journal of Raman spectroscopy*, 34(9), 642-650. Retrieved from: https://doi.org/10.1002/jrs.1045

Raman, C. V., Krishnan, K. S., (1928). A new type of secondary radiation. *Nature,* 121(3048), 501-502.

Serafetinides, A. A., Makropoulou, M., & Spyratou, E. (2013, March). Optical tweezers and cell biomechanics in macro-and nano-scale. In 17th International School on Quantum Electronics: Laser Physics and Applications (Vol. 8770, pp. 309-321). SPIE.

Shiomi, H., Tsuda, S., Suzuki, H., & Yomo, T. (2014). Liposome-based liquid handling platform featuring addition, mixing, and aliquoting of femtoliter volumes. *PLoS One*, 9(7), e101820. Retrieved from: https://doi.org/10.1371/journal.pone.0101820

Shitamichi, Y., Ichikawa, M., & Kimura, Y., (2009). Mechanical properties of a giant liposome studied using optical tweezers. *Chemical Physics Letters*, 479(4-6), 274-278. Retrieved from: https://doi.org/10.1016/j.cplett.2009.08.018

Simon, A., Libchaber, A. (1992). Escape and synchronization of a Brownian particle. *Physical review letters,* 68(23), 3375. Retrieved from: https://doi.org/10.1103/PhysRevLett.68.3375

Singer, W., Bernet, S., Hecker, N., & Ritsch-Marte, M. (2000). Three-dimensional force calibration of optical tweezers. Journal of Modern Optics, 47(14-15), 2921-2931.

Spyratou, E., Cunaj, E., Tsigaridas, G., Mourelatou, E. A., Demetzos, C., Serafetinides, A. A., Makropoulou, M. (2015). Measurements of liposome biomechanical properties by combining line optical tweezers and dielectrophoresis. Journal of Liposome Research, 25(3),202-210.

Stiles, P. L., Dieringer, J. A., Shah, N. C., & Van Duyne, R. P., (2008). Surface-enhanced Raman spectroscopy. *Annu. Rev. Anal. Chem.,* 1, 601-626. Retrieved from: https://doi.org/10.1146/annurev.anchem.1.031207.112814

Svoboda, K., Schmidt, C. F., Schnapp, B. J., & Block, S. M. (1993). Direct observation of kinesin stepping by optical trapping interferometry. *Nature,* 365(6448), 721-727.

Tolić-Nørrelykke, I. M., Berg-Sørensen, K., & Flyvbjerg, H. (2004). MatLab program for precision calibration of optical tweezers. *Computer physics communications*, 159(3), 225-240. Retrieved from:https://doi.org/10.1016/j.cpc.2004.02.012

Tukova, A., & Rodger, A. (2021). Spectroscopy of model-membrane liposome-protein systems: complementarity of linear dichroism, circular dichroism, fluorescence and SERS. Emerging Topics in Life Sciences, 5(1), 61-75.

Viana, N. B., Rocha, M. S., Mesquita, O. N., Mazolli, A., Neto, P. M., & Nussenzveig, H. M. (2007). Towards absolute calibration of optical tweezers. Physical Review E, 75(2), 021914.

Zhang, H. (2017). Thin-film hydration followed by extrusion method for liposome preparation. *Liposomes: Methods and protocols*, 17-22.

Zhang, S., Gibson, L. J., Stilgoe, A. B., Nieminen, T. A., & Rubinsztein-Dunlop, H. (2019). Measuring local properties inside a cell-mimicking structure using rotating optical tweezers. Journal of Biophotonics, 12(7), e201900022.